INSTITUTO SUPERIOR TÉCNICO

UNIVERSIDADE DE LISBOA

PROJETO INTEGRADOR DE 1º CICLO

Axisymmetric coil winding surfaces for non-axisymmetric nuclear fusion devices

Author:
João BIU

Supervisor:
Prof. Rogério JORGE

Research work performed for the Bachelor in Engineering Physics

at

Instituto de Plasmas e Fusão Nuclear
Physics Department

June 16, 2023

Abstract

Stellarators are nuclear fusion devices that confine plasma through non-axisymmetric magnetic fields. To create such fields, we need complex and precise coils, which are hard to build and expensive. Therefore, to simplify the configuration of Stellarator coils we implement in this report a method to create coil curves bounded to a coil winding surface (CWS), with the parameterization of the curve being the sum of a secular linear term with a Fourier series. Using this method, we study the individual optimization of coils parameterized to fixed winding surfaces. The degrees of freedom used in the optimization are the coefficient of the linear term and the Fourier coefficients of each coil parameterization equation and along with the currents in each coil. This approach is used to study the viability of using a CWS resulting from rescaling the plasma boundary surface and comparing it with using a circular toroidal CWS with the same dimensions. As shown here, a lower plasma confining magnetic field error is obtained using coils parameterized in a surface rescaled from the plasma boundary rather than in a circular toroidal CWS.

1   Introduction

The climate crisis is, without doubt, one of the biggest problems faced nowadays, becoming irreversible and prominent to the planet each year that goes by. This problem is highly aggravated by the emission of greenhouse gases (GHG), to which the unsustainable use and production of energy heavily contribute. The energy sector is one of the main GHG emitters and their emissions keep increasing every year that goes by [1]. For these reasons, the energy sector needs to explore other means of energy production rather than keep using fossil fuels. The Intergovernmental Panel on Climate Change has indicated that an option to approach and eventually achieve zero GNG and CO_2 emissions is the transition from fossil fuels to low carbon energy sources [2]. However, the decarbonization of the electricity production sector is an expensive process. Furthermore, current renewable sources of energy may not be able to produce enough energy to cover the world's needs, nor be the best solution to reduce GNG emissions [3].

It is under these circumstances that nuclear fusion starts to grow as a viable candidate for a clean and safe way to produce energy to meet the world's increasing energy demand. Nuclear fusion occurs when two particles are brought together such that they overcome the electromagnetic repulsion between them and the strong force starts to act, in the scale of the particles' nuclei. From this process results a decrease of the mass Δm, therefore energy is released, according to $\Delta E = \Delta mc^2$. Even though nuclear fusion fuels the stars, it proves to be very difficult to achieve on Earth. To achieve nuclear fusion, high temperatures and a reaction with a large cross-section are needed, such as the fusion of deuterium and tritium, known as the D-T reaction,

$$_1^2D + {}_1^3T \longrightarrow {}_2^4He + n^0. \tag{1}$$

In such high temperatures matter exists in the plasma state, where the gas becomes fully ionized.

There are many ways to confine plasma. Since plasma is diamagnetic, it can be confined using magnetic fields in a process called magnetic confinement. Plasma at high temperatures can damage the walls of a reactor. Indeed, such damage is one of the main issues that must be accounted for in fusion devices. To prevent this from happening, we should analyze the behavior of the charged particles that constitute the plasma.

A charged particle has a helical trajectory along a field line when moving in a constant time-independent magnetic field. This can be used to trap a particle in the direction perpendicular to a field line. This field line is called the guiding center. Bending this field lines into a circle shape, thus creating a toroidal magnetic field, is the basis of toroidal confinement. But because the field decreases proportionally to the major radius of a torus, and an electric field is created from the charged particles of the plasma, a drift appears that makes the particles hit the vessel wall [4]. Therefore, a purely toroidal magnetic field cannot confine a plasma.

Tokamaks and Stellarators are two types of toroidal magnetic confinement fusion devices that solve the drift in charged particle motion when interacting with a magnetic and an electric field by creating field lines that twist around the magnetic flux surfaces, as shown in Fig. 1 (left). These are surfaces where the magnetic field is only tangent to. This way, the drift will change direction along the particle motion, being the mean drift along a closed trajectory zero. Tokamaks are axisymmetric and have a magnetic toroidal field created by external coils and a poloidal field that is created by inducing a toroidal plasma current, resulting in field lines that are toroidal helices. As a major advantage with respect to Tokamaks, Stellarators do not need an external current applied to the plasma, they can be run in a steady state.

However, Stellarators create field lines twisted around the surfaces by breaking axisymmetry, which can be done by having a non-planar magnetic axis, or by making the flux surfaces rotate poloidally along the toroidal angle [5]. This proves to be one of the biggest challenges for building Stellarators since the coils needed to create non-axisymmetric flux surfaces are usually expensive, difficult to design and build since they are generally non-circular and non-planar and have low tolerances, and there are numerous configurations that achieve the same magnetic field. Therefore, coil optimization is used to obtain the best possible coils that create the desired fields while minimizing construction difficulties, and this can be done in various ways. In this report, we will do a new approach to this subject by implementing a class in the Stellarator optimization framework SIMSOPT [6] in order to create and optimize coils parameterized to a coil winding surface with the goal of reducing the costs of building coils, by restricting the position of the coils.

2 Materials and Methods

To confine a plasma, the first step is to obtain a magnetic field capable of doing it. This magnetic field equilibrium can be achieved by solving the static ideal magnetohydrodynamics (MHD) system of equations. This system of equations combines Maxwell's electromagnetic equations with fluid dynamics, considering that plasma is a single fluid and a perfect electrical conductor without resistivity, with $\mathbf{E} + \mathbf{v} \times \mathbf{B} = 0$.

Ideal MHD relates the magnetic field $\mathbf{B}$, with the plasma current $\mathbf{J}$ density and the plasma pressure gradient ∇p in a set of equations given by

$$\mathbf{J} \times \mathbf{B} = \nabla p. \tag{2}$$

By solving this system of equations, we can obtain a magnetic field that confines the plasma and obeys Maxwell's equations, namely $\nabla \times \mathbf{B} = \mu_0 \mathbf{J}$ and $\mathbf{B} = 0$.

Ideal MHD is valid assuming a high collisionality regime and characteristic frequencies higher than the electron and ion gyro frequencies [7]. We can conclude from the force balance equations, Eq. (2), that $\mathbf{B}$ and $\mathbf{J}$ vectors are coincident with constant ∇p surfaces, as

$$\mathbf{B} \cdot \nabla p = \mathbf{J} \cdot \nabla p = 0, \tag{3}$$

showing that flux surfaces have constant pressure. Poicaré Index Theorem then implies that a magnetic field that confines a plasma must have a toroidal topology [8]. The necessary magnetic field for plasma confinement is one with flux surfaces nested inside each other.

Although nested surfaces are not guaranteed by the ideal MHD model, we obtain the $\mathbf{B}$ field using VMEC (Variational Moments Equilibrium Code) [9], which solves the MHD equations assuming a toroidal domain for the equilibrium solution, and assumes nested flux surfaces. VMEC obtains the MHD equilibrium by minimizing the potential energy of the plasma using the steepest descent method. The potential energy W is found by integrating Eq. (2) over a volume V, yielding
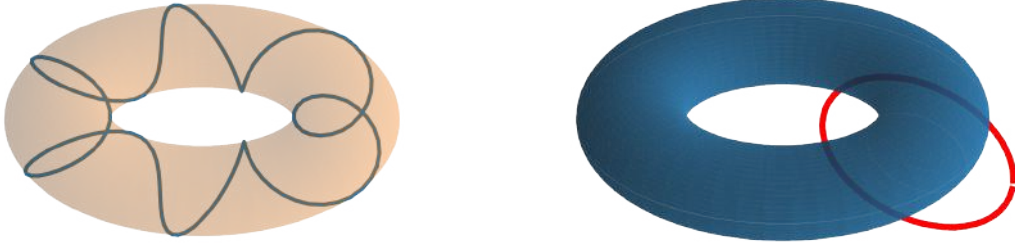
FIGURE 1: Left: Poloidally twisted fieldline along the toroidal angle, with a rotational transform of 1/6. Right: Surface (in blue) and curve (in red) made from Fourier Coefficients. $\mathbf{X}_{surface} = [1, 0.37, 0.37]$ and $\mathbf{X}_{curve} = [1, 0, 0.7, 0, 0, 0, 0, 0.7, 0]$.

$$W = \int \left(\frac{|B|^2}{2\mu_0} + \frac{p}{\gamma - 1} \right) d^3 x, \tag{4}$$

where γ is the adiabatic index (5/3 for a mono-atomic gas). The result is a boundary flux surface in the form of coefficients of a Fourier series, over a field period. This outermost flux surface is given in cylindrical coordinates, in the form

$$R(\theta, \phi) = \sum_{m=0}^{m_{pol}} \sum_{n=-n_{tor}}^{n_{tor}} \text{RBC}_{m,n} \cos\left(m\theta - n_{fp} n \phi\right), \tag{5}$$

$$Z(\theta, \phi) = \sum_{m=0}^{m_{pol}} \sum_{n=-n_{tor}}^{n_{tor}} \text{ZBS}_{m,n} \sin\left(m\theta - n_{fp} n \phi\right), \tag{6}$$

where $\theta \in [0, 2\pi[$ is a poloidal angle, $\phi \in [0, 2\pi[$ is the standard cylindrical angle and n_{fp} is the number of field periods. $\text{RBC}_{m,n}$ and $\text{ZBS}_{m,n}$ are the Fourier coefficients, and since we are working with surfaces that are symmetric under rotation by π about the x-axis, i.e., have Stellarator-symmetry, the sine term for R and the cosine term for Z are necessarily zero. The position vector for the surface is then given in cylindrical coordinates as $\mathbf{x} = [(R(\theta, \phi) \cos(\phi), R(\theta, \phi) \sin(\phi), Z(\theta, \phi)]$. The Fourier coefficients are $\mathbf{X}_{surface} = [\text{RBC}_{m,n}, \text{ZBS}_{m,n}]$. In the same way that surfaces are parameterized by (ϕ, θ), the external coils that create the magnetic field can be considered as curves parameterized by a single parameter. We can write the coordinates of the curve as

$$x(\theta) = \sum_{m=0}^{order} x_{c,m} \cos(m\theta) + \sum_{m=1}^{order} x_{s,m} \sin(m\theta), \tag{7}$$

with $\theta \in [0, 2\pi[$. The parameterization equation for $y(\theta)$ and $z(\theta)$ are analogous to Eq. (7). This way, to create coils, we only need to know the Fourier coefficients, in the form of $\mathbf{X}_{curve} = [x_{c,0}, x_{s,1}, x_{c,1}, \cdots, x_{s,order}, x_{c,order}, y_{c,0}, y_{s,1}, y_{c,1}, \cdots]$. Hence recreating coils and surfaces becomes an easy task to complete computationally, with the advantage that a function given by a Fourier series is continuous and differentiable, and we can calculate the analytical derivatives rather easily, instead of being required to rely on numerical methods such as finite differences. An example of a surface and a curve created from their Fourier coefficients can be found in Fig. 1 (right).

Once we get a suitable set of nested flux surfaces (described by their outer boundary) for the magnetic confinement of plasma, the optimization of the external coils that generate the desired magnetic field can also be done using optimization codes such as REGCOIL [10], FOCUS [11] or SIMSOPT [6]. In this work, we will use the SIMSOPT code.

SIMSOPT is a framework for Stellarator optimization, written in C++ and in Python, that does

both the optimization of the boundary flux surface (stage one) and the optimization of coils with the purpose of finding the coil geometry that creates the desired boundary surface (stage two). In the SIMSOPT code, coils are defined as parameterized curves with coordinates given by Fourier series, as explained previously. The degrees of freedom for the optimization are the Fourier coefficients and the current applied to each coil. The optimization is done by minimizing an objective function J that takes into account the quadratic flux, defined as the surface integral over the target plasma flux surface of the square of the magnetic field created by the coils normal to the surface.

$$J = \frac{1}{2} \int \frac{|\mathbf{B} \cdot \mathbf{n}|^2}{|\mathbf{B}|^2} d^2 x. \tag{8}$$

If the magnetic field induced by the coils and the target surface are coincident, this integral evaluates to zero. Additional coil regularization terms can be taken into account with different weights to the optimization, such as the coil length, curvature, torsion, coil-to-coil distance, and coil-to-surface distance. In order to study the optimization of coils in a coil winding surface, we will use SIMSOPT, as well as SciPy [12], for the minimization of the objective function J.

3 Results

To study the optimization of coils in a coil winding surface (CWS), the first thing that must be addressed is the parameterization of a curve in a surface. When defining a surface using Eqs. (5, 6), this task resumes to parameterizing θ and ϕ to the same parameter t. Since we want a closed curve, $\theta(t)$ and $\phi(t)$ must be continuous functions and periodic, of period $\mathcal{P}$. Since sine and cosine functions, both have a 2π period, we need to guarantee that $\theta(t + \mathcal{P}) = \theta(t) + 2k\pi$, with k an integer, and the same for ϕ. Therefore, we use a linear term with $t \in [0, 2\pi[$. We then have

$$\theta(t) = \theta_l t + \sum_{k=0}^{order} \theta_{c,m} \cos(kt) + \theta_{s,m} \sin(kt), \tag{9}$$

$$\phi(t) = \phi_l t + \sum_{k=0}^{order} \phi_{c,m} \cos(kt) + \phi_{s,m} \sin(kt). \tag{10}$$

Where the order is the number of terms of the Fourier series. This way, it is possible to define $\theta(t)$ and $\phi(t)$ via the coefficient of the linear term and the Fourier coefficients,

$$\mathbf{X} = [\theta_l, \theta_{c,0}, \cdots, \theta_{c,order}, \theta_{s,0}, \cdots, \theta_{s,order}, \phi_l, \phi_{c,0}, \cdots, \phi_{c,order}, \phi_{s,0}, \cdots, \phi_{s,order}]. \tag{11}$$

These are also the degrees of freedom of the coil optimization. The expressions for $\theta(t)$ and $\phi(t)$ are then used as an input for R and Z, Eqs. (5, 6), so that the coordinates of a parameterized curve in a surface are $\mathbf{x} = \mathbf{x}(t) = [(R(\theta(t), \phi(t)) \cos(\phi(t)), R(\theta(t), \phi(t)) \sin(\phi(t)), Z(\theta(t), \phi(t))]$.

Since this type of curve does not exist in SIMSOPT, the initial step was to implement a class that allows the creation and optimization of curves parameterized to surfaces, CurveCWSFourier. To create a curve of this type we need the order of the Fourier series of the parameterizations described by Eqs. (9, 10), the number of quadrature points to compute the curve, and the degrees of freedom of the $\theta(t)$ and $\phi(t)$, in Eq. (11). We also need the parameters of the CWS, defined below. The example below shows how to initialize an object of CurveCWSFourier type.

```
from simsopt.geo import CurveCWSFourier
Curve = CurveCWSFourier(CWS.mpol, CWS.ntor, CWS.x, quadpoints=150, order=0,
    CWS.nfp, CWS.stellsym)
Curve.set_dofs([1, 0, 0, 0])
```
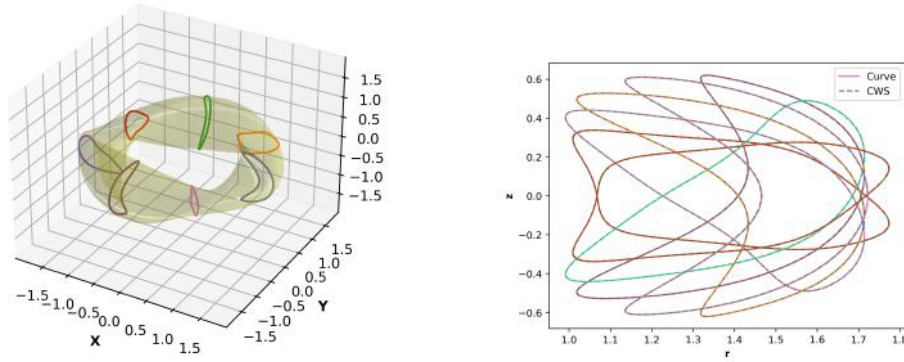
FIGURE 2: Left: Superimposed set of coils and CWS for the NCSX Stellarator. Right: Cross sections of the CWS (dashed lines) and curves at different toroidal angles ϕ (continuous lines). The CWS used for both is NCSX's plasma surface and the curves were generated using CurveCWSFourier.

In the class constructor *CWS.mpol* and *CWS.ntor* are the number of poloidal and toroidal modes of the CWS, respectively, *CWS.x* are the CWS degrees of freedom, *CWS.nfp* is the number of field periods and *CWS.stellsym* is its Stellarator-symmetry. The order of the Fourier Series of the curve parameterizations, Eqs. (9, 10) is given by *order*, and *quadpoints* is the number of quadrature points in the interval $[0, 2\pi[$ in which the curve coordinates are calculated.

In Fig. 2 (left) are shown CurveCWSFourier curves, using a non-axisymmetric CWS. This class creates curves by recomputing the surface from its Fourier coefficients, but using Eqs. (9, 10) instead of $\theta \in [0, 2\pi[$ and $\phi \in [0, 2\pi[$. This way we can guarantee curves on the surface and guarantee that the coordinates of the curves match the surface exactly, as shown in the right figure of Fig. 2. Other properties of the curves were defined, such as the first, second, and third derivatives of the curve coordinates, $\mathbf{x}(t)$, with respect to the parameter t, and the gradient of the coordinates with respect to the degrees of freedom defined in Eq. (11). The first derivative of the $x(t)$ with respect to t is given by:

$$
\frac{dx(t)}{dt} = \sum_{m=0}^{m_{pol}} \sum_{n=0}^{2n_{tor}} \left[-\text{RBC}_{m, n-n_{tor}} \sin\left(m\theta(t) - n_{fp}n\phi(t)\right) \left(m\frac{d\theta(t)}{dt} - n_{fp}n\frac{d\phi(t)}{dt} \right) \cos(\phi(t)) \right.
$$
$$
\left. -\text{RBC}_{m, n-n_{tor}} \cos\left(m\theta(t) - n_{fp}n\phi(t)\right) \sin(\phi(t))\frac{d\phi(t)}{dt} \right].
\tag{12}
$$

This was implemented in the files *curvecwsfourier.h* and *curvecwsfourier.cpp*. The expressions for $dy(t)/dt$ and $dz(t)/dt$ are analogous to Eq. (12). The derivatives of Eqs. (9, 10) with respect to t are $d\theta(t)/dt$ and $d\phi(t)/dt$. Using the secular linear term and a Fourier series for the parameterizations of θ and ϕ makes it rather easy to calculate the analytic expression of the derivatives.

The implementation of this class and its methods was validated by comparing the results obtained for the coordinates and derivatives of a CurveCWSFourier object with those of a CurveXYZFourier object, a curve class from SIMSOPT. To do this, curves with the same sizes, coordinates, and quadrature points were created using both classes, and the values of their methods were compared using the sum of absolute differences. The values obtained for the sum of the differences were of an order of 10^{-15}, proving that the implementation was successful. The deviation could be from the computational errors of calculation values of sine and cosine functions.

For the optimization of coils in a CWS in a Stellarator, a boundary surface was first obtained using Single-Stage Optimization [13]. This way we could obtain a magnetic field boundary surface for which the parameterization of the coils in a CWS was taken into account during stage one. This improves
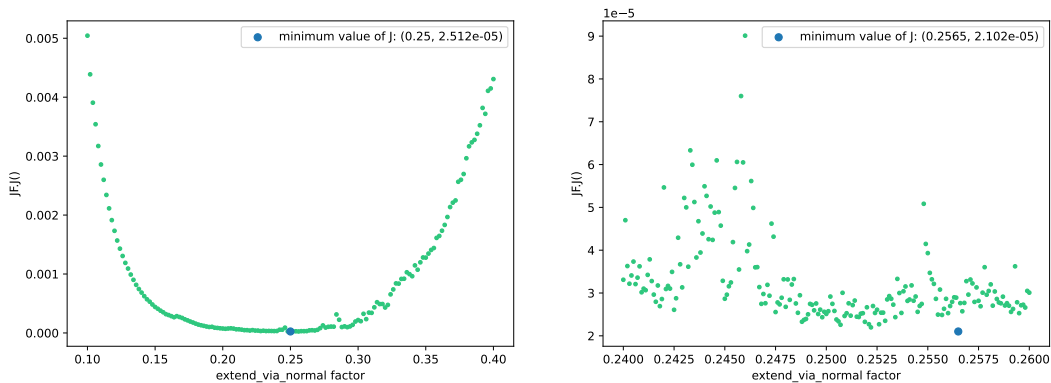
FIGURE 3: Result of the minimization of the objective function J for each value of the rescaling factor. Left: Varying RF in the interval from 0.1 to 0.4 meters with a step value of 2×10^{-3} m. Right: Varying RF in the interval from 0.24 to 0.26 meters with a step value of 1×10^{-4} m.

the quality of the optimization of CurveCWSFourier curves, compared to the optimization where the desired surface did not take the CWS in account. This surface was used for the multiple stage two optimizations done next. For the coil optimizations, we used 4 coils per number of field periods and an order of 10 for the Fourier series in Eqs. (9, 10). Our objective function J took into account the quadratic flux and additional terms with constraints such as the coil length ($l_{max} \leq 20$ m), the coil-to-coil distance ($d_{min} \geq 0.1$ m), the curvature of the coil ($\kappa_{max} \leq 60$ m^{-1}), and the mean quadratic curvature ($\kappa_{msc} \leq 60$ m^{-2}). The minimizations use the L-BFGS-B algorithm for which the analytic gradients are necessary.

In regard to the optimization of coils in a CWS, we first used a CWS resulting from the rescaling of the plasma surface, using the surface method implemented on SIMSOPT, *extend_via_normal(arg)*. The argument of this function is the distance from the original surface to the new rescaled surface used as CWS. We will address this increment as the rescaling factor (RF). Since the value of RF is the coil-to-surface distance, we decided to search for the value that minimizes J the most. To do this we did a sweeping where for each value of RF we ran the stage two optimization in order to find the value of RF that achieves the minimum value of J. The values of RF went from 0.1 to 0.4 meters with a step of 2×10^{-3} meters, and the minimizing value of RF found was 0.25 meters, as shown in Fig. 3 (left). Next, we did a new sweeping in the proximity of the minimum, varying RF between 0.24, and 0.26 meters with a step of 1×10^{-4} meters, as shown in Fig. 3 (right). The value of RF that best minimizes the objective function is RF = 0.2565 meters, for which J = 2.102×10^{-5}.

As we can observe in the left graph of Fig. 3, for RF values in the interval from 0.194 to 0.292 meters, J has a value in the order of 10^{-5}. Because of this, we expect to obtain good results for optimizations using these values of RF, and in the instance of building an optimized Stellarator, having a broad interval of possible coil-to-surface distances could be useful since that in this extra space instruments for diagnosis of the operation of the device can be implemented.

Using the magnetic field boundary surface obtained from the Single Stage and the value of RF that minimizes the value of J, for the stage two optimization of coils with a CWS created by rescaling the magnetic surface, we obtained the configuration shown in Fig. 4. For this optimization the values obtained were J = 4.723×10^{-6} and the quadratic flux (Eq. (8)) was 3.727×10^{-6}. Although the values obtained were small, in the order of 10^{-6}, we can conclude the effectiveness of the optimization using a CWS by analyzing the Poincaré Plot in Fig. 5, where we can verify that there is almost no deviation of field lines from the nested magnetic field surfaces computed using the MHD equilibrium code, VMEC. Poincaré plots are obtained by tracing the field lines generated by the coils and plotting the intersection of their trajectories with a plane at a given cylindrical toroidal angle.
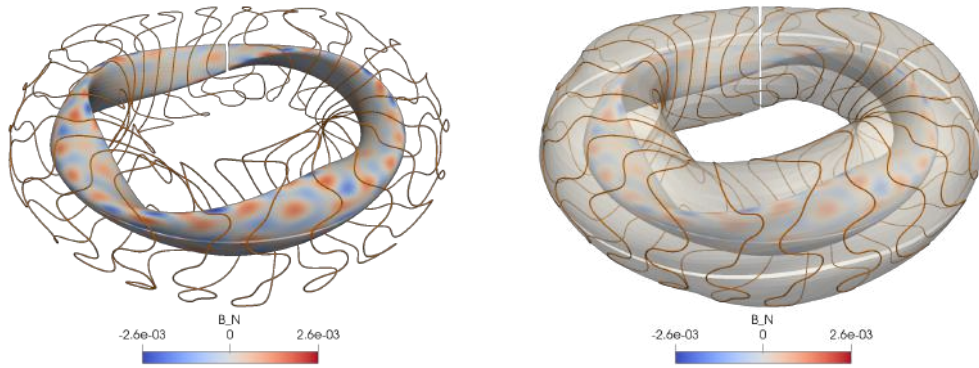
FIGURE 4: Result obtained from stage two optimization of coils in a CWS resulting from rescaling the magnetic field boundary surface. Left: Transparent CWS. Right: Visible CWS.
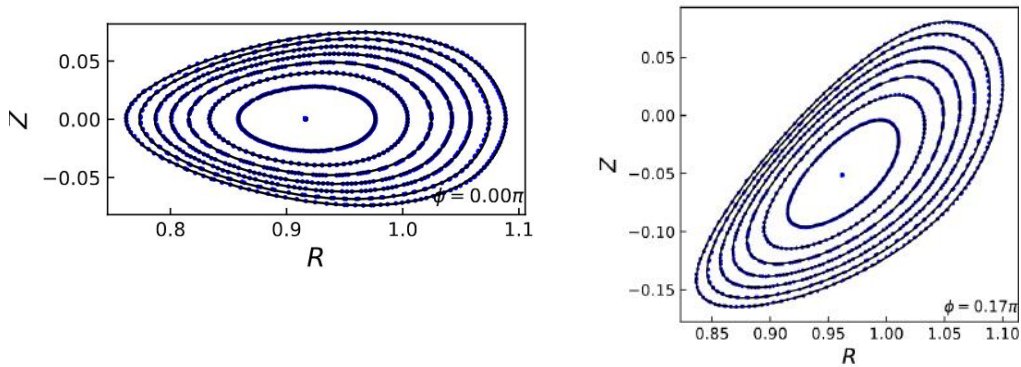

FIGURE 5: Superposition of magnetic surfaces at constant cylindrical toroidal angle ϕ of the surface obtained with Single-Stage optimization (lines), and the Poincaré plot resulting from tracing magnetic field lines created by the obtained CurveCWSFourier coils (dots). Left: $\phi = 0\pi$. Right: $\phi = 0.17\pi$.

Engineering-wise, to produce energy from nuclear fusion, there must be in the fusion device a component named blanket-and-shield between the plasma surface and the CWS. In this component, the cooling system responsible for capturing the heat from the fusion reaction is built. This heat will be used to produce electricity. The blanket-and-shield must be 1.2 meters thick [4], corresponding to the coil-to-surface distance. In our optimization, the coil-to-surface distance is RF = 0.2565 meters, with the major radius of the plasma boundary being normalized to 1 meter. Doing the rescaling, to have a coil-to-surface distance of 1.2 meters, the major radius of the magnetic field surface must be 4.678 meters, keeping the same proportionality. Our Stellarator would be smaller than Wendelstein 7-X, with a major radius of 5.5 meters.

To compare the result obtained previously with a circular toroidal CWS, we did an optimization using a torus whose small radius was the sum of the small radius of plasma boundary surface, given by the Fourier coefficient $ZBS_{1,0}$ from Eq. (6), and the value of RF used previously, 0.2565 meters, as shown in Fig. 6 (right). The value of J obtained was 3.344×10^{-5} and the quadratic flux was 2.887×10^{-5}. Comparing the values obtained, for a circular toroidal CWS, J was 10 times higher than the values obtained using a CWS rescaled from the plasma boundary surface. There are also magnetic
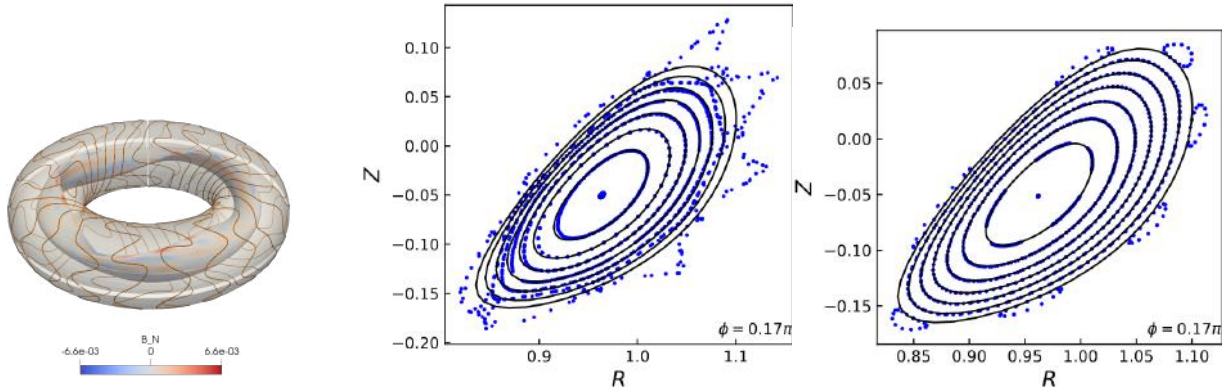
FIGURE 6: Left: Circular toroidal CWS. Center: Poincare Plots using a circular toroidal CWS. Right: Poincaré Plot using a CWS rescaled from the plasma boundary surface with RF = 0.2522 m.

islands interior and exterior to the boundary surface, and magnetic field lines deviating from the nested surfaces, as shown in the Poincaré plot for this optimization, in Fig. 6 (center). The magnetic island chain 3/7 seen in Fig. 6 stems from the fact that the rotational transform at the boundary is close to a rational number, namely 3/7 where 3 is the number of field periods and 7 the number of islands. Therefore, we conclude that the use of the CWS created from the rescaling of the plasma boundary has a better outcome than a circular toroidal one.

Another result worth noting is that using CWS rescaled from the plasma surface, with RF = 0.2522 meters, the value of J obtained is 5.516×10^{-6} and we obtain magnetic islands outside of the boundary surface, as shown in Fig. 6 (right). This value of RF was the second best value for the minimization of J obtained in the sweeping and this result is relevant because the magnetic islands could prove to be useful for implementing island divertors [14].

All the code written and results obtained supporting this study can be found on [15].

4   Conclusions

The implementation of CurveCWSFourier allows the optimization and study of Stellarators with coils parameterized to a specific winding surface. In the study done, we use this approach to optimize coils in two different surfaces, one resulting from the rescaling of the plasma boundary surface, and the other being a circular torus.

In regard to the use of a winding surface rescaled from the plasma boundary, from the agreement between the value obtained from the minimization of the objective function J, 4.723×10^{-6}, and the Poicaré plots in Fig. 4, we can conclude the effectiveness of the optimized configuration of parameterized coils in achieving the desired magnetic field. This is not the same case when using a circular toroidal coil winding surface. In this case, the optimization of the coils was not able to find a coil configuration that generated the desired field. The better results were obtained for a coil winding surface with more similarities to the plasma boundary, for example, having the same number of field periods as the boundary surface. It was also shown that the coil-to-surface distance when using a coil winding surface is an important parameter for achieving different configurations of the magnetic field, such as magnetic islands in the boundary surface. The behavior of the field for the values of RF where the optimization is expected to have better results, i.e., in the interval from 0.194 to 0.292 m, as shown in Fig. 3 (left) could be studied more deeply since the distance between the plasma and the coils is relevant to the building of the blanket-and-shield of a Stellarator.

Although we proved that it was possible to use coils parameterized to a winding surface to achieve a magnetic field close to the desired one, these coils will always be limited in terms of the coil-to-surface distance, since it depends only on the winding surface. This loss of freedom is compensated by the torsion of the coils, which proved to be higher than desired in the optimizations done. This will contribute to the complexity of the coil design, even parameterized to a rather simple CWS such as a circular torus, going against the goal of reducing the costs of production of coils.

Another future work to be done is the optimization of the coil winding surface simultaneously with the optimization of curves parameterized to it. Having non-fixed CWS could be beneficial by bringing more freedom for the shape of the coils, meaning more adaptability to the desired needs for achieving the best possible magnetic field. This could be allied with Single-Stage Optimization to optimize the plasma boundary, the coil winding surface, and the coils simultaneously, leading to become a powerful tool in the design of next-generation fusion reactors.

References

[1] J. C. Minx et al. "A comprehensive and synthetic dataset for global, regional, and national greenhouse gas emissions by sector 1970–2018 with an extension to 2019". In: *Earth System Science Data* 13.11 (2021), pp. 5213–5252.

[2] IPCC. "Climate Change 2023: Synthesis Report. A Report of the Intergovernmental Panel on Climate Change. Contribution of Working Groups I, II and III to the Sixth Assessment Report of the Intergovernmental Panel on Climate Change [Core Writing Team, H. Lee and J. Romero (eds.)]" In: (in press).

[3] Nuclear Energy Agency. *The Costs of Decarbonisation*. 2019, p. 224.

[4] J. Freidberg. *Plasma Physics and Fusion Energy*. Cambridge University Press, 2007.

[5] P. Helander et al. "Stellarator and tokamak plasmas: a comparison". In: *Plasma Physics and Controlled Fusion* 54 (12 2012), p. 124009.

[6] M. Landreman et al. "SIMSOPT: A flexible framework for stellarator optimization". In: *Journal of Open Source Software* 6 (65 2021), p. 3525.

[7] J. Freidberg. *Ideal MHD*. Cambridge University Press, 2014.

[8] P. Helander. "Theory of plasma confinement in non-axisymmetric magnetic fields". In: *Reports on Progress in Physics* 77 (8 2014), p. 087001.

[9] S. P. Hirshman et al. "Steepest-descent moment method for three-dimensional magnetohydrodynamic equilibria". In: *The Physics of Fluids* 26 (12 1983), pp. 3553–3568.

[10] M. Landreman. "An improved current potential method for fast computation of stellarator coil shapes". In: *Nuclear Fusion* 57 (4 2017), p. 046003.

[11] C. Zhu et al. "New method to design stellarator coils without the winding surface". In: *Nuclear Fusion* 58 (1 2017), p. 016008.

[12] P. Virtanen et al. "SciPy 1.0: Fundamental Algorithms for Scientific Computing in Python". In: *Nature Methods* 17 (2020), pp. 261–272.

[13] R. Jorge et al. "Single-stage stellarator optimization: combining coils with fixed boundary equilibria". In: *Plasma Physics and Controlled Fusion* 65 (7 2023), p. 074003.

[14] E. Strumberger. "SOL studies for W7-X based on the island divertor concept". In: *Nuclear Fusion* 36 (7 1996), p. 891.

[15] *CurveCWSFourier Optimization*. GitHub repository at `https://github.com/joaopedrobiu6/CurveCWSFourier_Optimization`.